eLife

Reviewed Preprint
v1 • May 14, 2026
Not revised

For correspondence:
ledan@post.bgu.ac.il

Competing interests: No competing interests declared

Reviewing editor: Xiaobing Shi, Van Andel Institute, United States



# SETD6-mediated methylation of PPARγ establishes a transcriptional feedback circuit promoting lipid accumulation in liver-derived cells

**Noa Nashnaz[1], Dana Goldberg[1], Maayan Abramov[1], Anand Chopra[1], Habib Muallem[2], Yulia Haim[2], Michal Feldman[1], Assaf Rudich[2], Dan Levy[1]**

[1]The Shraga Segal Department of Microbiology, Immunology and Genetics, Faculty of Health Sciences, Ben-Gurion University of the Negev, Beer-Sheva, Israel • [2]Department of Clinical Biochemistry and Pharmacology, Faculty of Health Sciences, Ben-Gurion University of the Negev, Beer-Sheva, Israel

## eLife Assessment

This is an **important** study uncovering a new role of the SETD6-PPARγ axis in the regulation of hepatic lipid metabolism. The data **convincingly** demonstrate that methylation of PPARγ by SETD6 plays a key role in this process, linking lysine methylation to transcriptional control of lipid storage genes.

https://doi.org/10.7554/eLife.111542.1.sa2

## Abstract

Nonalcoholic fatty liver disease (NAFLD) is characterized by excessive accumulation in hepatocytes and affects approximately 25% of the global population. The nuclear receptor PPARγ is a central regulator of lipid storage and metabolic gene expression in the liver; however, how post-translational modifications modulate its transcriptional activity remains incompletely understood. Here, we identify lysine methylation as a regulatory mechanism controlling PPARγ function. We show that the lysine methyltransferase SETD6 directly binds to and mono-methylates PPARγ at lysine 170 within its DNA-binding domain. This modification enhances PPARγ occupancy at target gene promoters and promotes the expression of lipid metabolism genes.

Mechanistically, SETD6-mediated methylation of PPARγ facilitates its recruitment to chromatin and is required for full transcriptional activation of key lipid droplet-associated genes, including MOGAT1 and PLIN2. In turn, PPARγ directly activates SETD6 transcription in a methylation-dependent manner, establishing a positive feedback circuit that amplifies lipid metabolic gene expression. Transcriptomic analysis reveals that both SETD6 and PPARγ K170 methylation regulate overlapping gene networks enriched for lipid metabolism pathways. Functionally, disruption of SETD6 or mutation of PPARγ at K170 impairs lipid droplet accumulation in hepatocytes.

Together, our findings uncover a previously unrecognized post-translational modification of PPARγ that regulates its chromatin binding and transcriptional activity, and define a SETD6–PPARγ regulatory axis that promotes hepatic lipid accumulation. These results provide new insight into epigenetic control of metabolic gene expression and suggest potential therapeutic targets for NAFLD.

## Introduction

Nonalcoholic fatty liver disease (NAFLD) is a highly prevalent metabolic disorder characterized by excessive lipid accumulation in hepatocytes, primarily in the form of lipid droplets (1). These dynamic organelles serve as the major intracellular storage sites for neutral lipids and play a central role in maintaining cellular lipid homeostasis. Dysregulated lipid droplet biogenesis and expansion are key features of NAFLD progression and are tightly controlled by transcriptional programs. Among these, the nuclear receptor PPARγ is a major regulator of lipid uptake and storage, promoting the expression of genes involved in lipid droplet formation and metabolism (RED). While PPARγ activity is modulated by ligand binding and post-translational modifications, the mechanisms that fine-tune its transcriptional function at chromatin remain incompletely understood.

Lysine methylation, among other well-studied post-translational modifications (PTMs), is emerging as a critical player in the regulation of many cellular signaling pathways. The methylation of lysine residues is performed by protein lysine (K) methyltransferases (PKMTs) which can selectively catalyze mono-, di-, or tri-methylation (2). There are over 60 members of this enzyme family, the vast majority of which contain a conserved SET domain responsible for the enzymatic activity (2,3). The mono-methyltransferase SET domain–containing protein 6 (SETD6) is involved in the regulation of many cellular pathways through the methylation of non-histone proteins. These biological processes include the NFKB pathway, oxidative stress response, WNT signaling, cell cycle regulation, embryonic stem cell self-renewal among several others (4). Many of these pathways and processes have been implicated in metabolism and fatty liver diseases. However, the role of lysine methylation and protein lysine methyltransferases (PKMTs) in the regulation of non-histone proteins in lipid droplet formation and steatosis remains largely unexplored.

PPAR family members are ligand-activated nuclear receptors that function as transcription factors. The family consists of three PPAR isotypes: PPARα, PPARβ/δ, and PPARγ, with highly conserved DNA and ligand binding domains (5,6). The DNA binding domain enables the binding to consensus DNA sequences called peroxisome proliferator response elements (PPREs), usually found in the promoter region of genes (7). Despite their similar domain structure and mechanism of action, PPARs are encoded by different genes and activated by different ligands. PPARα is highly expressed in oxidative tissues, such as the liver, skeletal muscle, brown adipose tissue, heart, and kidney (8). It mainly participates in the fasting state and regulates the transcription of rate-limiting enzymes required for peroxisomal and mitochondrial beta-oxidation (8). PPARβ/δ is ubiquitously expressed and has mainly been studied in skeletal muscle (9). Similar to PPARα, it has been shown to have anti-inflammatory effects (10). PPARγ has two main isoforms – PPARγ1 and PPARγ2 (11). PPARγ — and specifically PPARγ2 (from here on referred to as PPARγ) — appears to be the major isoform expressed in hepatocytes, where it contributes to fat accumulation and lipid droplet formation. Transcriptional activation of PPARγ in the liver facilitates the uptake of free fatty acids from circulation and stores them in lipid droplets (11).

Here, we identify a previously unrecognized role for SETD6 in regulating lipid droplet accumulation in liver cells. We show that SETD6 directly binds to and methylates PPARγ at lysine 170 (K170) on chromatin. This modification enhances PPARγ occupancy at target gene promoters and promotes the transcription of genes involved in lipid droplet formation. Mechanistically, SETD6-mediated methylation of PPARγ is required for efficient lipid droplet accumulation in hepatocytes. In addition, we uncover a positive feedback circuit in which PPARγ directly activates SETD6 expression in a SETD6– and K170 methylation-dependent manner. Together, our findings define a SETD6–PPARγ regulatory axis that links lysine methylation to transcriptional control of lipid metabolism, thereby contributing to hepatic steatosis and highlighting SETD6 as a potential regulator of NAFLD progression.

# Results

## *SETD6* is a target gene of PPARγ in HepG2 cells

PPARγ has previously been shown to bind to a PPRE in the *SET7/9* promotor and enhance its transcription (12). Interestingly, using the JASPAR CORE database (13), we identified a significant predicted Peroxisome Proliferator Response Element (PPRE) within the promoter region of *SETD6* (Fig. 1A). This putative PPRE binding site implies that PPARγ may regulate SETD6 expression through binding to the SETD6 promoter. Analysis of publicly available ChIP-sequencing experiments (14), of liver HepG2 cells, where PPARγ is highly expressed (15), revealed that PPARγ is indeed enriched at the *SETD6* promoter region in an open chromatin state (ATAC-seq), along with an enrichment for the histone marks H3K4me3 and H3K27ac in that genomic region (Fig. 1B). To determine whether PPARγ binds to putative PPRE within the promoter of *SETD6*, we performed a chromatin immunoprecipitation (ChIP) experiment to evaluate the occupancy of the PPARγ in HepG2 cells in this genomic region. As shown in Figure 1C, we could identify a significant enrichment of Flag-PPARγ at the *SETD6* promoter. Consistent with these results, over-expression of PPARγ resulted in a significant elevation in SETD6 mRNA expression level that was measured by qPCR (Fig. 1D). To test the possibility that the observed occupancy on the *SETD6* promoter and its activation by PPARγ is direct, we cloned the full-length *SETD6* promoter upstream to a luciferase reporter gene (16), followed by transfection of this luciferase reporter construct and Flag-PPARγ in HepG2 cells. We found a significant elevation in *SETD6* promotor activity after over-expression of Flag-PPARγ (Fig. 1E). Consequently, these results demonstrate that PPARγ binds to *SETD6* promoter and activates its transcription.

## SETD6 binds and methylates PPARγ at K170 *in-vitro* and in cells

We have previously shown that SETD6 methylation of the transcription factor E2F1 positively regulates the expression level of SETD6 (16). We hypothesized that a similar mechanism may occur also with SETD6 and PPARγ. To address this hypothesis, we first tested if there is a direct physical interaction between SETD6 and PPARγ. An *in-vitro* ELISA experiment using purified recombinant proteins confirmed a direct SETD6-PPARγ interaction. MBP-RelA served as positive control (17,18) and BSA and PBS were used as negative controls for these experiments (Fig. 2A). Further, Over-expression of Flag-PPARγ and HA-SETD6 followed by a FLAG IP from HepG2 chromatin also demonstrated an interaction (Fig. 2B). Further, endogenous SETD6 was immunoprecipitated from the chromatin fraction of HepG2 cells to assess the endogenous interaction. Compared to the condition without SETD6 antibody, PPARγ was enriched after SETD6 immunoprecipitation, thereby indicating these two endogenous proteins interact on chromatin (Fig. 2C). Finally, and consistent with previous results, we confirmed the physical interaction between GFP-SETD6 and endogenous PPARγ in the HepG2 cell nuclei using a proximity ligation assay (PLA) (Fig. 2D). Given the physical interaction between SETD6 and PPARγ *in-vitro* and in cells, we hypothesized that PPARγ is methylated by SETD6. To address this hypothesis, recombinant PPARγ was subjected to an *in-vitro* methylation reaction using His-SETD6 and $^{3}$H –labeled SAM as the methyl donor. The results show that SETD6 methylates PPARγ (Fig. 3A, **lanes 1-3**). To map the methylation site, *in vitro* methylation reactions were performed using non-radioactive SAM followed by mass spectrometry. The data obtained from the MS suggested (Spectra is shown in Fig. S1), that PPARγ K170 mono-methylation (located in the DNA binding domain (DBD)) was the only methylation site identified after incubation with SETD6. A schematic illustration of the DBD of PPARγ and the estimated location of K170 is shown (Fig. 3A, **top panel**). To validate this methylation site, we performed an *in-vitro* methylation reaction using a PPARγ with a K170R mutation. SETD6 could not induce the methylation of mutant PPARγ (Fig. 3A, **lanes 4-5**). Therefore, K170 is the major methylation site of PPARγ by SETD6. Immunoprecipitation with a pan-methyl antibody confirmed that endogenous PPARγ is methylated in HepG2 cells on chromatin (Fig. 3B). To test if this methylation is SETD6-dependent, we compared the methylation of Flag-PPARγ in CRISPR control (CT) and SETD6 knockout (KO) cells. The result revealed that Flag-PPARγ is methylated in cells in a SETD6-dependent manner (Fig. 3C). We next generated a site-specific antibody to detect PPARγ

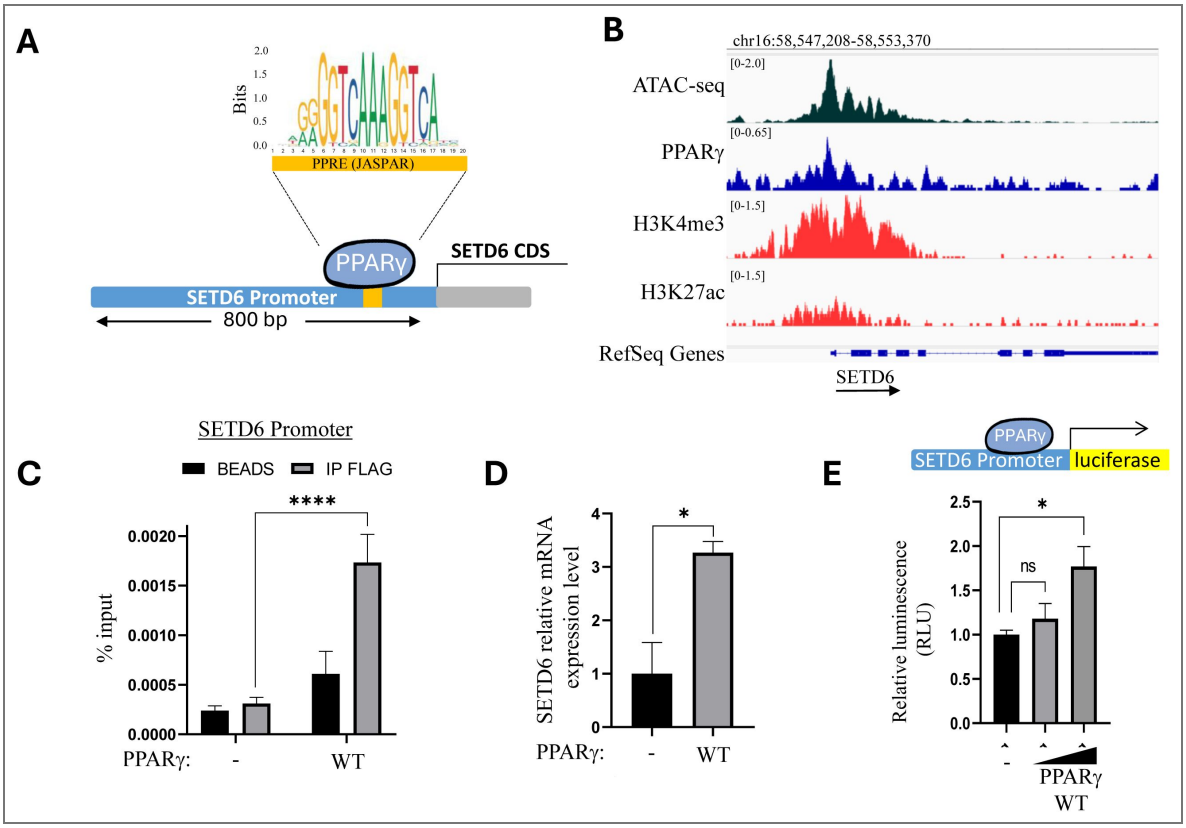


**Figure 1. PPARγ binds SETD6 promoter and activates its expression.**

**(A)** Top: Sequence logo of the PPARγ response element (PPRE) from JASPAR. Bottom: Schematic representation of PPARγ binding to a predicted PPRE site within the SETD6 promoter **(B)** Capture of a genome browser showing the enrichment of PPARγ at the SETD6 promoter in HepG2 cells with open chromatin state represented by H3K4me3, H3K27ac, and ATAC-seq tracks. **(C)** ChIP assay with Flag-PPARγ antibody or beads as negative control in HepG2 cells followed by qPCR with primers flanking the predicted binding site at the SETD6 promoter. Graphs show % input of the quantified DNA. **(D)** RNA was extracted from HepG2 cells transfected with control or Flag-PPARγ WT. Transcript levels of SETD6 were determined by qPCR. Error bars are SEM. Statistical analysis was performed for three experimental repeats using one-way ANOVA (*p < 0.05, ****p < 0.0001). **(E)**– dual-luciferase assay in HepG2 cell transfect with an increasing amount of Flag-PPARγ. About 24 h post-transfection, the whole cell lysates were subjected to dual-luciferase assay (Promega). Relative luminescence was calculated after normalization of the firefly luciferase signal over Renilla luciferase control. Error bars are SD. Statistical analysis was performed for three experimental repeats. *p ≤ 0.03

K170me1. In a dot blot experiment we can validate that the PPARγ K170me1 antibody recognizes a PPARγ peptide mono-methylated at K170 but not the un-modified version (Fig. 3D). To test if PPARγ is methylated in cells, we immunoprecipitated endogenous PPARγ from HepG2 cells in CRISPR CT and SETD6 KO cells followed by WB with the PPARγ K170me1 antibody. A significant decrease in PPARγ methylation was observed in the SETD6 KO cells (Fig. 3E). Taken together, these results revealed that SETD6 binds and methylates PPARγ on K170 at chromatin *in vitro* and in cells.

## PPARγ methylation at K170 regulates SETD6 promoter activation

Having demonstrated that PPARγ binds to the *SETD6* promoter and activates its transcription, we hypothesized that a molecular feedback mechanism may exist whereby SETD6-mediated methylation of PPARγ at K170 influences SETD6 transcription. To test this hypothesis, we performed a luciferase reporter-based assay to determine *SETD6* promoter activity in control and SETD6 KO cells in the presence of over-expressed Flag-PPARγ. As shown in Figure 4A, we found a significant decrease in the promotor activity in the SETD6 KO cells. To complement these experiments, we measured SETD6 mRNA levels by qPCR in HepG2 cells stably expressing either Flag-PPARγ WT or the Flag-PPARγ K170R mutant. A significant elevation in SETD6 mRNA expression level was observed in cells overexpressing WT PPARγ compared with the PPARγ K170R mutant (Fig. 5B). To determine whether the occupancy of PPARγ on the *SETD6* promotor is SETD6-dependent we performed ChIP experiments of endogenous PPARγ in HepG2 crispr CT and SETD6 KO cells (Fig. 5C). The ChIP experiments revealed that SETD6 KO led to a significant reduction in the occupancy of PPARγ on the SETD6 promoter. To test if the occupancy of PPARγ on the *SETD6* promoter is K170me1-dependent, we performed a ChIP experiment in cells stably expressing Flag-PPARγ WT and Flag-PPARγ K170R mutant (Fig. 5D). The enrichment of Flag-PPARγ was significantly higher in the cells expressing PPARγ WT compared to the K170R mutant. Taken together, the results suggest that PPARγ binds to the *SETD6* promoter and activates SETD6 mRNA expression in a SETD6– and a K170me1-dependent manner, thereby demonstrating a positive feedback loop.

## PPARγ K170 methylation by SETD6 regulates mediates lipid droplets formation

To assess whether SETD6 has a more widespread role in transcriptional regulation in liver hepatocellular carcinoma, we performed RNA-sequencing experiment comparing the expression signature of hepatic HepG2 control cells (2 independent gRNAs) and SETD6 knock-out (KO) cells (derived from 3 independent gRNAs). The KO efficiency of SETD6 gRNAs in these cells is shown in Fig. 5A. RNA-seq analysis revealed 302 differentially expressed genes, whereby 166 and 136 genes were downregulated or upregulated, respectively (Fig. 5B). Notably, KEGG enrichment analysis revealed the significant enrichment of genes involved in lipid metabolism, as well as other related cancer– and stem cell-related pathways which are consistent with previous reports of SETD6-mediated regulation. (4) (Fig. 5C). Interestingly, the KEGG analysis also identified an enrichment of the PPAR signaling pathway, which further supports the functional link between SETD6 and PPARγ in liver hepatocellular carcinoma. To phenotypically validate whetherSETD6 has a role in fat accumulation, we established a live cell imaging system that allows us to quantify and study the kinetics of lipid droplet accumulation in live cells (Fig. 5D). In this system, we treat HepG2 with oleic acid (OA), as the primary fatty acid source followed by staining with BODIPY 493/503, a green-fluorescent dye that stains neutral lipids (19). Hoechst dye was used to identify the nuclei and quantify the number of cells, enabling a calculation of mean green fluorescence over time. First, we performed a calibration experiment for 20 hours to determine the appropriate OA concentration (Fig. S2). We incubated HepG2 cells with three different concentrations of OA; 300, 600 and 900 μM, and with DMSO serving as a vehicle control. OA accumulation in the cells treated with 300 μM and 600 μM reached a plateau over time. The DMSO-treated cells exhibited a decline in LD accumulation, indicating that the BODIPY dye is specific to neutral lipid staining. We chose to work with the 600uM concentration of OA since it yielded

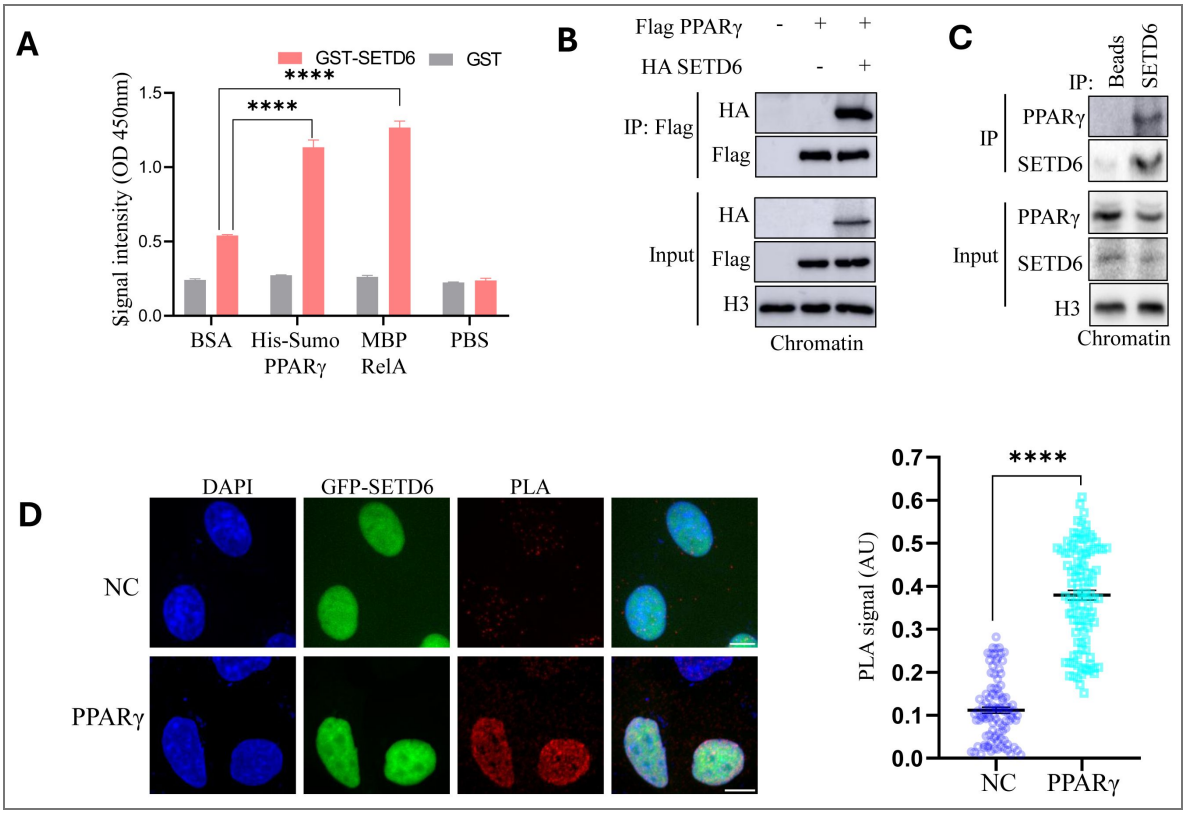


**Figure 2. Physical interaction between PPARγ and SETD6 in-vitro and in cells**

**(A)** ELISA-based analysis of the interaction between recombinant GST-SETD6 and the indicated recombinant proteins. ****p < 0.0001. **(B)** HEK293T cells were transfected with the indicated plasmids followed by immunoprecipitation with Flag antibody of the chromatin fraction. Samples were then subjected to WB analysis using the indicated antibodies. **(C)** Endogenous SETD6 was immunoprecipitated from chromatin isolated from HepG2 cells followed by western blot with the indicated antibodies. **(D)** Left-Representative images of PLA detecting GFP-SETD6 and Flag-PPARγ proximity in HepG2 cells. Red dots represent PLA signal. Scale bar = 10 micron. Right-PLA signal quantification for each sample. Statistical analysis was performed using student's t-test (**** p<0.0001).

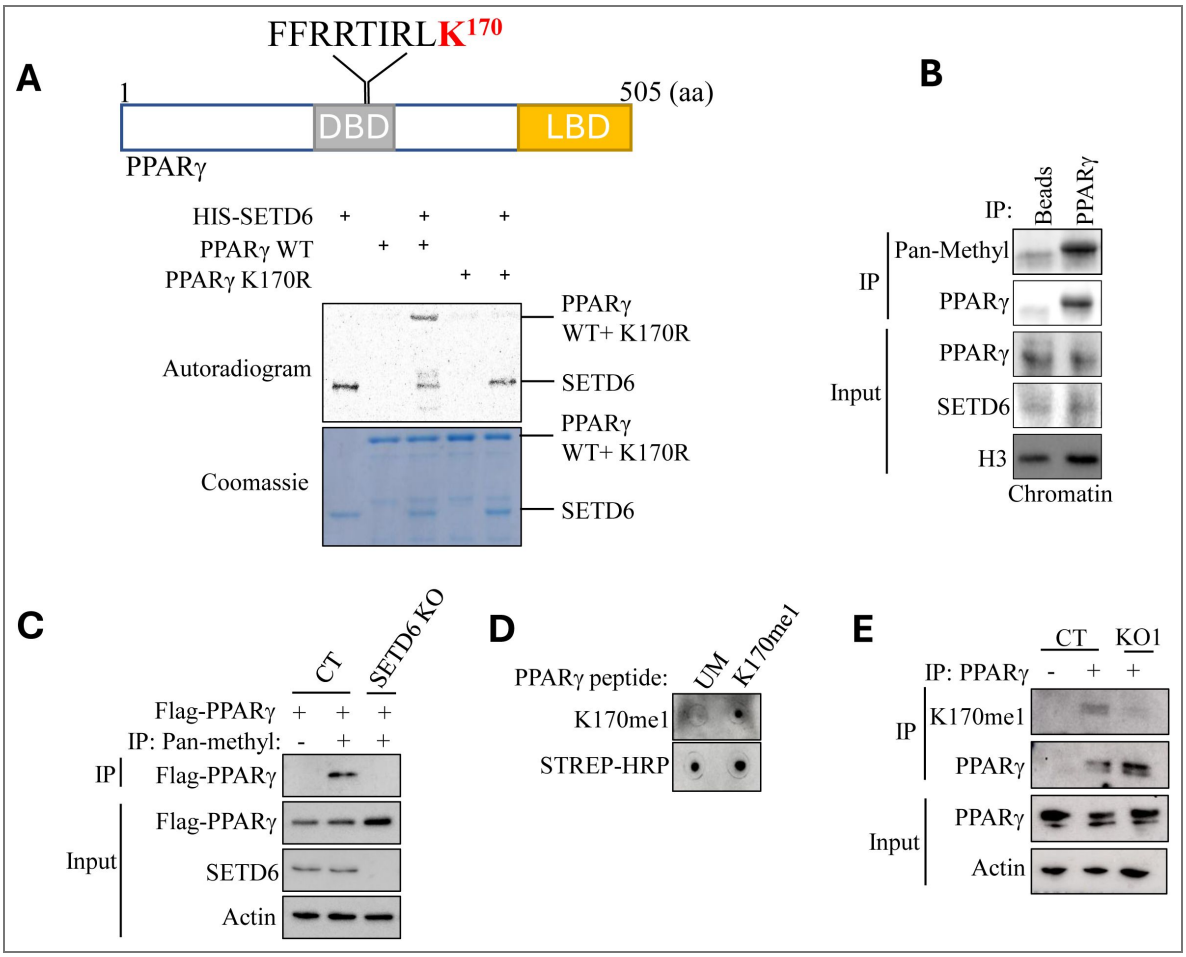


**Figure 3. SETD6 methylates PPARγ at K170 in-vitro and in cells.**

**(A)** *In vitro* methylation assay in the presence of $^{3}$H-labeled SAM and the indicated purified proteins. Coomassie stain of the recombinant proteins used in the reactions is shown at the bottom. Schematic representation of PPARg domain structure. The methylated residue (K170) identified by mass spectrometry is shown in red. DBD-DNA binding domain; LBD-ligand binding domain. **(B)** Endogenous PPARγ was immunoprecipitated from HepG2 cells followed by WB with the indicated antibodies **(C)** Flag-PPARγ was over-expressed followed by immunoprecipitation using pan-methyl antibody in control (CT) and SETD6 KO cells followed by western blot with indicated antibodies. **(D)** 0.25ug of PPARγ peptides (un-modified and K170me1) were spotted on a nitrocellulose membrane followed by incubation with anti-PPARγ K170me1 antibody or Streptavidin-HRP. **(E)** Endogenous PPARγ was immunoprecipitated from control and KO SETD6 HepG2 cells followed by western blot with the indicated antibodies.

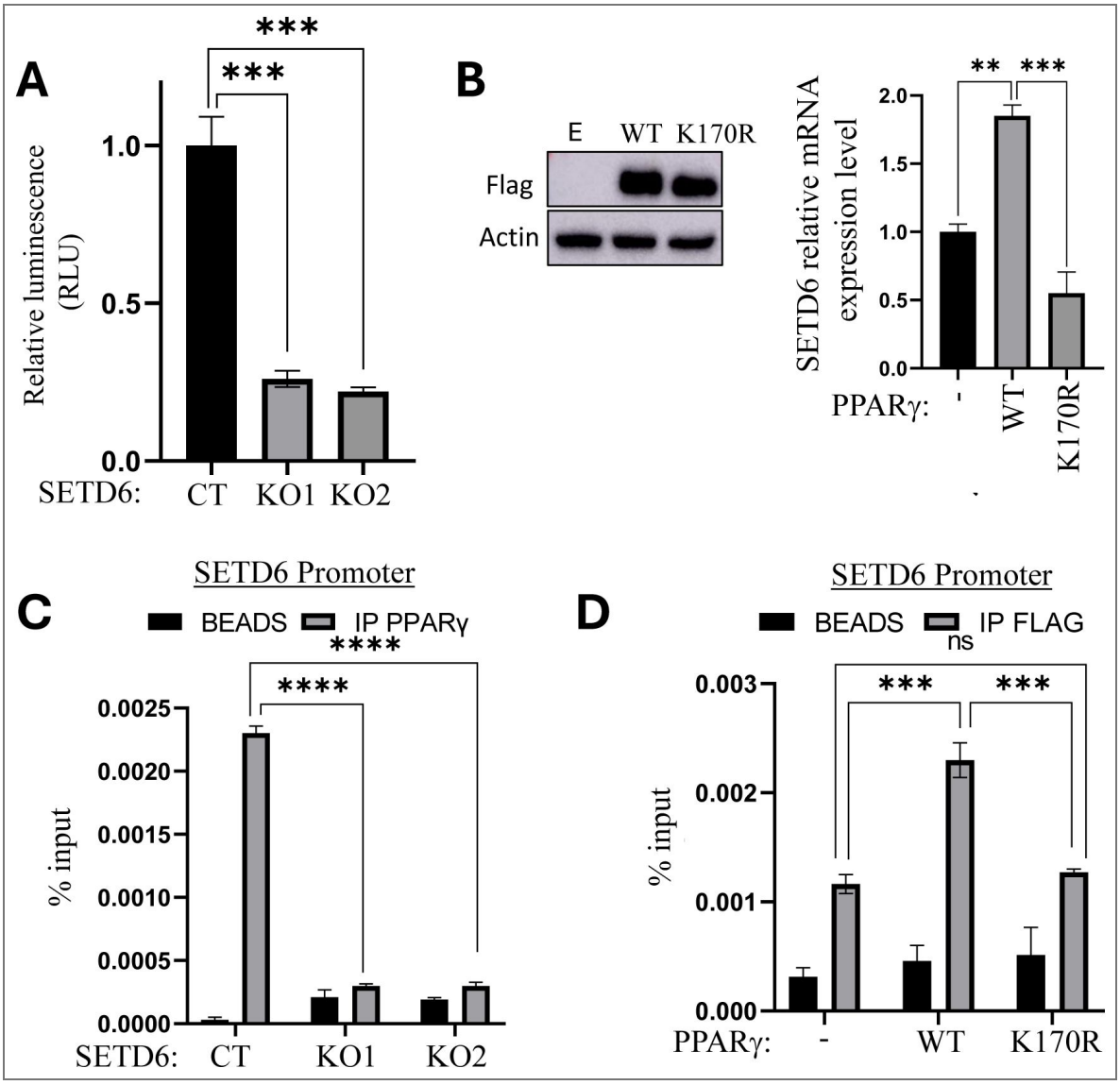


**Figure 4. PPARγ binds and activates SETD6 expression in a K170 methylation dependent manner**

**(A)** – dual-luciferase assay in Control and SETD6 KO HepG2 cells. 24 h post-transfection, the whole cell lysates were subjected to dual-luciferase assay (Promega). Relative luminescence was calculated after normalization of the firefly luciferase signal over Renilla luciferase control. Error bars are SD. Statistical analysis was performed for three experimental repeats. ***$p < 0.001$. **(B)** Left-WB analysis with the indicated antibodies for stable cells expressing Flag-WT or Flag-K170R PPARγ. Right-Transcript levels of the SETD6 were determined by qPCR of stably expressing HepG2 cells-Empty, Flag-PPARγ WT, and Flag-PPARγ K170R mutant. mRNA levels were normalized to GAPDH and then to Empty. **(C)** Chromatin immunoprecipitation (ChIP) assay. The chromatin fraction of HepG2 SETD6 CRISPR CT, KO1, and KO2 cells were immunoprecipitated with magnetic beads conjugated with anti-PPARγ antibody. The bound DNA was purified and amplified by qPCR. **(D)** Same as C for cells stably expression of Empty, Flag-PPARγ WT, and Flag-PPARγ K170R mutant. Graphs for C and D show the percent input of the quantified DNA. Two-way ANOVA analysis was performed; error bars are S.E.M. *$p < 0.05$; **$p < 0.01$; ***$p < 0.001$; ****$p < 0.0001$.

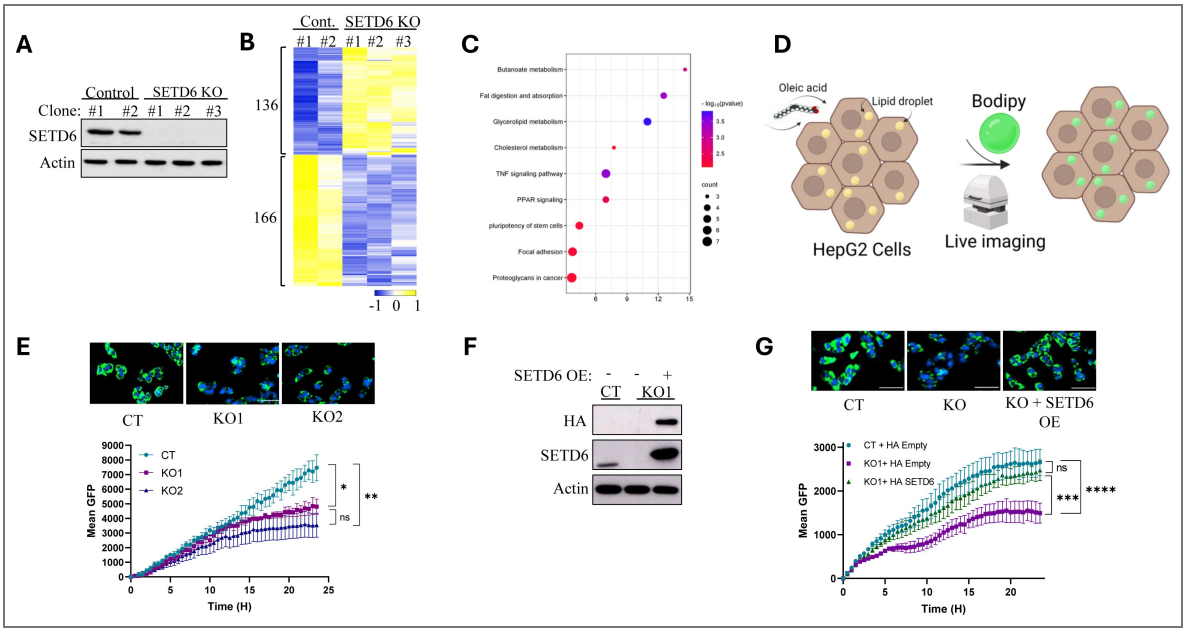


**Figure 5. SETD6 positively regulates lipid droplets formation:**

**(A)** WB analysis with the indicated antibodies for HepG2 control (2 clones) and SETD6 KO cells (3 clones) **(B)** Heatmap showing up– and down-regulated genes from RNA-sequencing analysis of 2 SETD6 control and 3 KO HepG2 cells independent clones. Yellow and blue colors represent high and low expression levels, respectively. **(C)** Selected pathways from gene ontology (GO) analysis of the differentially expressed genes were analyzed. Circle size represents the count of differentially expressed genes related to each pathway. **(D)** Illustration of the system to monitor lipid droplets accumulation over time: HepG2 cells are treated with oleic acid (OA) and stained with Hoechst (nucleus) and BODIPY (neutral lipids), followed by live cell imaging. **(E)** Top-Representative images of HepG2 CRISPR CT (control), KO1, and KO2 challenged with 300 mM of OA (20 H time point) and stained with Hoechst (nucleus) and BODIPY (neutral lipids). Bottom-Mean green fluorescence was calculated as fluorescence signal divided by cell count. Data is analyzed from three beacons per well in three wells. Statistical analysis was performed using one-way ANOVA. ns: non-significant; *p < 0.05; **p < 0.01. **(F)** WB analysis for CT and SETD6 KO with or without over-expression of HA-SETD6. **(G)** Top-Representative images of HepG2 CRISPR CT (control) and SETD6 KO without or with over-expression of HA-SETD6, challenged with 300 mM of OA (20 H time point) and stained with Hoechst (nucleus) and BODIPY (neutral lipids). Bottom-Mean green fluorescence was calculated as fluorescence signal divided by cell count. Data is analyzed from three beacons per well in three wells. Statistical analysis was performed using one-way ANOVA. ns: non-significant; ***p < 0.001; ****p < 0.0001.

optimal staining conditions and did not affect the cell morphology. We next asked if depletion of SETD6 affects the formation of lipid droplets in cells? To this end, HepG2 CT and KO SETD6 cells were treated with 600uM of OA over 24 hours, and the mean GFP signal was measured. The result shows that the CT cells accumulated significantly more lipid droplet over time compared to SETD6 KO1 and KO2 cells (Fig. 5E). Representative images of HepG2 CRISPR CT, KO1, and KO2 cells at a 24-hour time point are presented (Fig. 5E, top panel). To confirm that the lipid droplets accumulation is dependent on SETD6, we performed a rescue experiment wherebySETD6 KO cells were transfected with HA-SETD6 plasmid (Fig. 5F). The results showed that exogenous HA-SETD6 expression reversed the effect of SETD6 knockout. These findings suggest that SETD6 is a positive regulator of lipid droplet formation.

Given that SETD6 methylates PPARγ as well as positively regulates lipid droplet formation, we hypothesized that this phenotype is mediated by PPARγ K170 methylation and its transcriptional activity. We next sought to understand if SETD6 methylation on PPARγ K170 regulates HepG2 gene expression profile. To this end we performed RNA-sequencing with HepG2 cells stably expressing Flag-PPARγ WT and Flag-PPARγ K170R mutant (Fig. 6A). We identified 1122 differentially expressed genes, whereby 590 were downregulated and 532 were upregulated. Interestingly, KEGG enrichment analysis revealed a significant elevation in the expression of genes involved in lipid metabolism in cells stably expressing PPARγ WT compared to cells stably expressing PPARγ K170R mutant (Fig. 6B). These results are consistent with the enriched pathways identified by RNA-seq analysis in control and SETD6 KO cells (Figure 5B). The RNA-seq results were further validated by qPCR (Fig. S3). Taken together, this data demonstrates that methylation of PPARγ at K170 positively regulates the expression of genes associated with lipid droplet formation. The fact that K170 is in the DNA binding domain of PPARγ, may suggest that the methylation affect its association with target genes linked to lipid droplets formation. To test this hypothesis, we decided to focus on two PPARγ target genes, that are known to be involved in the LD formation process; MOGAT1 – a rate-limiting enzyme involved in incorporating fatty acids into triglycerides and characterizes the fatty-acid esterification step (20), and PLIN2 – surrounds the lipid droplet and is involved in assisting the storage of neutral lipids within the lipid droplets (21). ChIP experiments revealed that PPARγ is significantly more enriched at the MOGAT1 and PLIN2 loci in the SETD6 CT cell line compared to the SETD6 KO cells (Fig. 6C). Consistent with these results, using HepG2 stables cell lines we observed a greater enrichment of FLAG-PPARγ WT on the both MOGAT1 and PLIN2 promoter regions in comparison the FLAG-PPARγ K170R mutant (Fig. 6D). Finaly, to test if lipid droplet formation is dependent onPPARγ methylation at K170 we have subjected the cells to the live imaging system described earlier. The result shows significantly less accumulation of lipid droplets in cells expressing Flag-PPARγ K170R compared to Flag-PPARγ WT (Fig. 6E). These results strongly suggest that K170 PPARγ methylation positively mediates lipid droplet formation. Taken together, we propose a working model in which SETD6 methylates PPARγ at lysine 170 (K170), enhancing its transcriptional activity on target genes involved in lipid droplet formation, including *MOGAT1* and *PLIN2*. This activation promotes lipid droplet accumulation. In parallel, PPARγ K170 methylation drives the transcription of *SETD6*, establishing a positive feedback loop that sustains the expression of LD-associated genes.

## Discussion

Previous studies have shown that PPARγ undergoes post-translational modifications such as phosphorylation, acetylation, ubiquitination, and sumoylation (22–26). Interestingly, a recent paper has shown that SMYD2 mono methylation of PPARγ facilitates hypoxia-induce pulmonary hypertension and promotes mitophagy (27) However, no methylation site has been reported. Herein, we found the first evidence that uncovered a link between SETD6 and lipid droplet formation. Specifically, we identified SETD6 as a novel enzymatic regulator of PPARγ transcriptional activity by inducing lysine methylation of its DBD. Our data demonstrate that SETD6 methylates PPARγ at K170 to positively regulate the expression of *SETD6* transcription and as well as fundamental genes associated with lipid droplet formation.

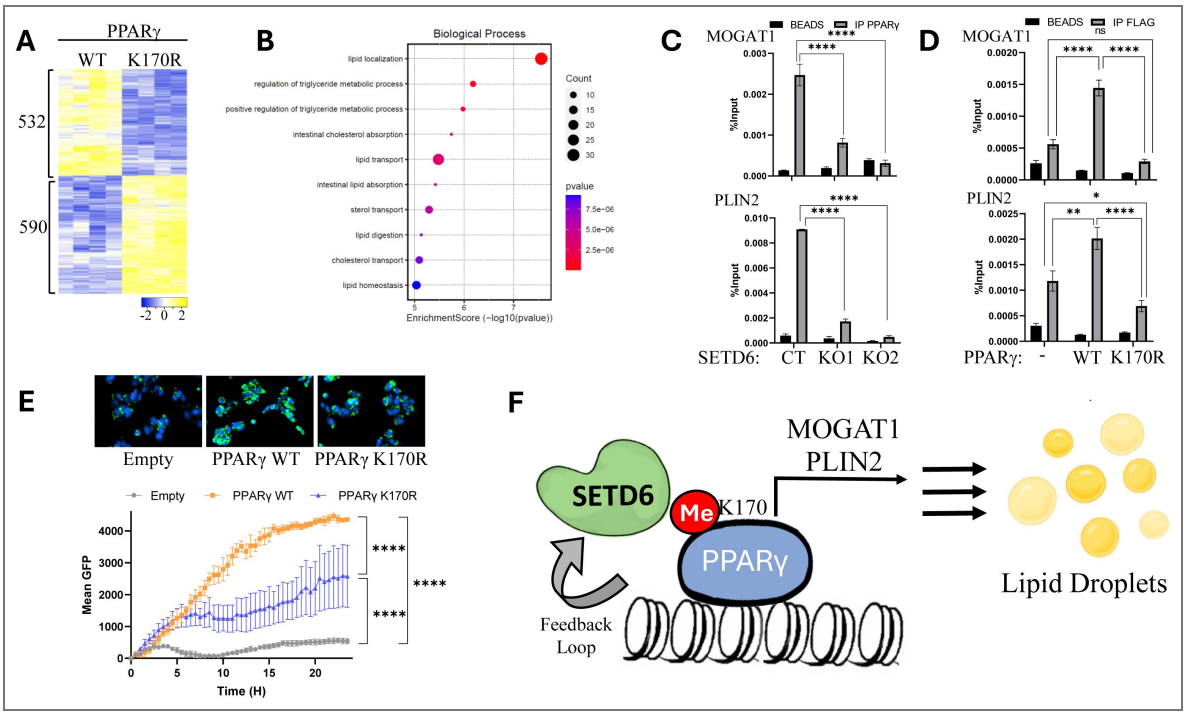


**Figure 6. PPARγ methylation at K170 positively regulates gene expression and lipid droplets formation.**

**(A)** Heatmap showing up– and down-regulated genes from RNA-sequencing analysis of HepG2 cells stably expression PPARg-WT and PPARg K170R mutant. independent clones. Yellow and blue colors represent high and low expression levels, respectively. **(B)** Selected pathways from gene ontology (GO) analysis of the differentially expressed genes were analyzed. Circle size represents the count of differentially expressed genes related to each pathway. **(C)** ChIP analysis for HepG2 control and SETD6 KO cells (two clones) that were immunoprecipitated with PPARg antibody. The bound DNA was purified and amplified by qPCR using specific primers to MOGAT1 and PLIN2 gene promoter regions. Graphs show the percent input of the quantified DNA. Two-way ANOVA analysis was performed; error bars are S.E.M. ****p < 0.0001. **(D)** Same as for C with HepG2 cells stably exprssing Empty, Flag-PPARγ2 WT, and Flag-PPARγ2 K170R mutant that were immunoprecipitated with FLAG conjugated magnetic beads. error bars are S.E.M. ns: non-significant; *$p < 0.05$; **$p < 0.01$; ****$p < 0.0001$. **(E)** Top-Representative images of HepG2 cells stably expressing Empty, PPARγ WT or PPARγ K170R mutant, challenged with 300 mM of OA (20 H time point) and stained with Hoechst (nucleus) and BODIPY (neutral lipids). Bottom-Mean green fluorescence was calculated as fluorescence signal divided by cell count. Data is analyzed from three beacons per well in three wells. Statistical analysis was performed using one-way ANOVA. ****p < 0.0001. **(F)** A Schematic representation of our proposed working model.

ChIP-sequencing analysis performed on HepG2 cells revealed that PPARγ is enriched in the promoter region of the *SETD6* gene. This observation suggested a potential feedback loop mechanism whereby PPARγ may regulate SETD6 expression. Our findings demonstrate that SETD6-mediated methylation of lysine 170 (K170) on PPARγ affects the occupancy of this transcription factor on the *SETD6* promoter region, thereby influencing *SETD6* gene expression in a positive feedback loop mechanism. Specifically, methylation of PPARγ at K170 enhances its occupancy at the SETD6 promoter, leading to an upregulation of SETD6 transcription and an increase in SETD6 mRNA levels. Our results not only suggest that PPARγ positively regulates the expression of SETD6 but also provides evidence that it occurs in a SETD6– and a PPARγ methylation-dependent manner. In our previous work we demonstrated that SETD6 methylates E2F1 at K117, and that E2F1 methylation positively regulates the expression of SETD6 mRNA. While our knowledge about the upstream signals which regulate SETD6 gene expression is limited, it seems that it has to be controlled in a delicate manner to allow the tight regulation of the enzymatic activity of SETD6.

Our RNA sequencing analysis of stably expressing HepG2 cells with wild-type PPARγ and the PPARγ K170R mutant provided insight into the functional consequences of SETD6-mediated methylation on PPARγ in various biological processes. Specifically, we observed that methylation at lysine 170 (K170) positively regulates the expression of genes associated with lipid metabolism, particularly those involved in lipid droplet formation. These findings highlight the critical role of PPARγ methylation in modulating metabolic pathways linked to lipid storage and processing. Given that the K170 methylation site is located within the DNA-binding domain (DBD) of PPARγ, specifically between its two zinc-finger motifs, we investigated how this post-translational modification affects the occupancy of PPARγ at its target gene promotors. Our analysis focused on its binding to peroxisome proliferator response elements (PPREs) present in the promoter regions of key target genes, including MOGAT1 and PLIN2 (28,29).

Consistent results were observed in both SETD6 CRISPR knockout cells and overexpression models. PPARγ exhibited significantly greater enrichment in the promoter regions of control SETD6 CRISPR cells (in comparison to SETD6 KO) and cells stably expressing Flag-PPARγ WT cells (compared to Flag-PPAR K170R mutant). These findings demonstratethat the methylation of PPARγ at K170 by SETD6 facilitates its recruitment to promoter region of its target genes. The increased transcriptional activity of MOGAT1 and PLIN2 likely drives their protein expression, thereby contributing to lipid accumulation within cells via their known functions. A broader investigation into additional PPARγ target genes that may be affected by SETD6 expression and K170 methylation is required to further understand whether our finding reflect a global phenomenon

Lysine K170 on PPARγ is conserved among the other PPAR family member, PPARβ/δ but not in PPARα. These findings may suggest that the other PPAR family members which have other physiological roles in different tissues, can be potentially regulated by SETD6 and methylation in a similar way. Future experiments will allow us to determine whether the newly identified methylation event is redundant or is specific just to PPARγ.

Base on the Phosphosite database it seems that K170 in PPARγ was not found to be modified by an additional type of modification such as acetylation and ubiquitination. Interestingly, T166 which is in a close proximity to K170 and also located at the DNA binding domain, was shown before to be phosphorylated by PKCalpha. T166 phosphorylation was shown to modulate the transcriptional activity of PPARγ and to program lipid metabolism processed in adipocytes (30). These findings, which require further investigation, may suggest for a potential methylation/phosphorylation cross talk which results in competition or synergism in the regulation of PPARγ transcription activity.

Future studies should involve the usage of mouse models, where high-fat diet (HFD) and low-fat diet (LFD) fed mice serve as standard models for investigating fatty liver disease and NAFLD. This *in vivo* approach will allow us to evaluate the effects of diet-induced conditions on the entire liver and organism mimicking physiological conditions to further validate the mechanistic models

suggested in this paper. Using such models will allow us to study the role of SETD6-mediated K170 methylation of PPARγ, focusing on genomic alterations, as well as the progression of steatosis and inflammation in mice expressing either wild-type PPARγ or the K170R mutant.

In summary, this study highlights the pivotal cellular role of SETD6 and its lysine methylation activity. Our findings uncover a previously unrecognized function of SETD6 in promoting lipid droplets accumulation, mediated through its influence on the DNA-binding capacity and transcriptional regulation of PPARγ target genes in a methylation dependent manner. Integrating the data obtained in this study will pave new research directions to gain more insight into SETD6 role metabolic diseases through the methylation of PPARγ with potential therapeutic applications.

# Materials and Methods

## Cell lines treatment

HepG2 (Hepatocellular Carcinoma) cells were maintained in Eagle's Minimum Essential Medium (EMEM) (BI, 01-025-1A) with 10% fetal bovine serum (FBS) (Gibco, 10270106), 2 mg/ml L-glutamine (Sigma, G7513) and 1mM sodium pyruvate (BI, 03-042-1B). Human embryonic kidney cells (HEK-293T) cells were maintained in Dulbecco's modified Eagle's medium (DMEM) (Sigma, D5671) with 10% fetal bovine serum (Gibco, 10270106), 2 mg/ml L-glutamine (Sigma, G7513),1% penicillin-streptomycin (Sigma, P0781), and non-essential amino acids (Sigma, M7145). Cells were cultured at 37°C in a humidified incubator with 5% $CO_2$.

## Plasmids

Mouse PPARγ2 (mPPARγ2) coding sequence was excised from plasmids that were kindly provided by Yosef Shaul's lab from Weizmann Institute of Science. In addition, the human PPARγ2 (hPPARγ2) coding sequence was amplified from a sample of cDNA sequence from human visceral adipose tissue that was kindly provided by Prof. Assaf Rudich's lab. mPPARγ2 and hPPARγ2 sequences were amplified by using PCR with compatible primers as indicated in Table 1. The amplicons were digested with AscI and PacI restriction enzymes and mPPARγ2 subcloned into a pET-Sumo plasmid for protein purification. mPPARγ2 and hPPARγ2 subcloned into pcDNA3.1 3xFlag. To generate mPPARγ2 and hPPARγ2 mutants, site-directed mutagenesis on a PPARγ2 wild-type vector was performed for each plasmid using other primers indicated in Table 1. PPARγ2 K170R mutants were also cloned into pcDNA3.1 3xFlag, and mPPARγ2 K170R mutant was cloned into a pET-Sumo plasmid for protein purification. PCR reactions were accomplished using the KAPA HiFi HotStrart ReadyMix (KAPA Biosystems), and cloned plasmids were confirmed by sequencing. Cloning pET-Duet and pcDNA3.1 hSETD6 (Human) plasmid containing His and HA tags described in (31), respectively. *SETD6* promoter sequence was amplified by PCR using primers indicated in table 1, and subcloned into pGL3 plasmid.

| Name | Sequence (5’ to 3’) |
|---|---|
| mPPARγ2-fw | TTAGGCGCGCCGGTGAAACTCTGGGAGATTCTCC |
| mPPARγ2-rev | GGCTTAATTAACTAATACAAGTCCTTGTAGATCTCCTGG |
| mPPARγ2-K170R-fw | GAACCATCCGATTGCGCCTTATTTATGATAGGTGTGATCTTA GCCG |
| mPPARγ2-K170R-rev | CTATCATAAATAAGGCGCAATCGGATGGTTCTTCGGAAAAA |
| hPPARγ2-AscI-fw | TAAGGCGCGCCGGTGAAACTCTGGGAGATTCTCC |
| hPPARγ2-PacI-rev | GGCTTAATTAACTAGTACAAGTCCTTGTAGATCTCCTGC |
| hPPARγ2-K170R-fw | GAACAATCAGATTGCGCCTTATCTATGACAGATGTGATCTT AACTGTCGG |
| hPPARγ2-K170R-rev | TCTGTCATAGATAAGGCGCAATCTGATTGTTCTCCGGAAGA AACC |
| SETD6 promoter-fw | TTAGGTACCAACCTCTATATTCACAGCCTC |
| SETD6 promoter-rev | GGCCAAGCTTGTTCTGCGAACGGAGAAG |
| SETD6 gRNA #1 | TAAGGCGCGCCGGTGAAACTCTGGGAGATTCTCC |
| SETD6 gRNA #2 | GGCTTAATTAACTAGTACAAGTCCTTGTAGATCTCCTGC |

**Table 1.** **Primers for cloning and mutagenesis**

| Name | Sequence (5’ to 3’) |
|---|---|
| GAPDH FW | AGCCACATCGCTCAGACAC |
| GAPDH Rev | GCCCAATACGACCAAATCC |
| Mogat1 FW | GGAAAGCCATCCACACTGTT |
| Mogat1 Rev | CCTCCATATAGGTCTGATGTAACTCC |
| Mogat2 FW | GGTATCTGGACCGAGACAAGCC |
| Mogat2 Rev | GTGGAAGCCCGCAATGTAGTT |
| PLIN1 FW | ACATTAAAGGGAAGAAGTTGAAGC |
| PLIN1 REV | TTCTCCTGCTCAGGGAGGT |
| PLIN2 FW | TCAGCTCCATTCTACTGTTCACC |
| PLIN2 REV | CCTGAATTTTCTGATTGGCACT |
| PLIN4 FW | AGTTCCAAGCCAGGGACAC |
| PLIN4 REV | CTGCTGGGCCTTTTCAATC |
| PLIN5 FW | GATCACTTCCTGCCCATGAC |
| PLIN5 REV | CACCGAACCCACTTCAGG |
| SETD6 FW | GGATGAAAAGGAGCCCAACT |
| SETD6 BC | CTACCATCCGAAGACAATTCG |

**Table 2.** **Primers for qPCR**

## Transfection

Cells were plated in 10-cm plates, and transfection was performed using polyethyleneimine (PEI) reagent (Polyscience Inc., 23966) for HEK293T cells or Mirus reagents, TransIT-X2 or TransIT-LT1 for HepG2 cell line, according to the manufacturer's instructions. For stable transfection in HepG2 cell lines, retroviruses were produced by transfecting HEK293T cells with the indicated pLenti constructs (empty, Flag PPARγ2 wild-type or Flag PPARγ2 K170R) and with plasmids encoding PMD2 and PX3. Target cells were infected with the viral supernatants and selected with 4 μg/ml puromycin.

## SETD6 knock-out by CRISPR/CAS9

HepG2 CRISPR/Cas9 SETD6 knock-out cells were generated with four different sgRNAs for SETD6 that were cloned to the lentiCRISPR plasmid (Addgene, #49535). $3*10^5$ HepG2 cells per 6 well-plate were plated and transfected with Mirus reagent, TransIT-X2 for HepG2 cell line, according to the manufacturer's protocol. Following transduction and puromycin selection, single clones were isolated and expanded.

## Recombinant protein expression and purification

Escherichia coli BL21 transformed with a plasmid expressing a protein of interest were grown in LB media. Bacteria were harvested by centrifugation after IPTG induction and homogenized with ice-cold lysis buffer containing phosphate-buffered saline (PBS), 10mM imidazole, 0.1% Triton X-100, 1mM PMSF, and one complete mini protease inhibitors tablet (Roche). After adding 0.25mg/ml lysozyme for 30 min, the lysates were subjected to sonication on ice (18% amplitude, 1 min total, 10 sec ON/OFF). The tagged fusion proteins were purified on a His-Trap column using AKTA Pure protein purification system (GE). Eluted with 0.5M imidazole in PBS buffer, followed by overnight dialysis (PBS, 10% glycerol). Recombinant GST-SETD6 was overexpressed and purified from insect cells as previously described in (17).

## In vitro methylation assay

The methylation assay reaction (total volume of 25 μl) contained 2 μg of His-Sumo mPPARγ2 wt, or K170R mutant proteins and 2 μg His-SETD6, 2mCi 3H-labeled S-adenosyl-methionine (SAM) (AdoMet, Amersham) and 5 μl of PKMT buffer (20mM Tris-HCl pH 8, 10% glycerol, 20mM KCl, 5mM MgCl2). The reaction tube was incubated overnight at 30°C. The reaction was resolved by SDS-PAGE for Coomassie staining (Expedeon, InstantBlueTM) and exposed to autoradiogram. For the non-radioactive (cold) methylation assay, 300 μM non-radioactive SAM was added (Abcam, ab142221).

## Enzyme-linked immunosorbent assay (ELISA)

2 μg of recombinant proteins (BSA, MBP-RelA, and His-Sumo mPPARγ2 wt) diluted in PBS were added to a sticky surface (Greiner Microlon) 96-well plate and incubated for 1 hr at RT followed by 3% BSA blocking in PBST for 1hr incubation at RT. After 3 washes with PBST, the plate was covered with 0.5 μg GST-SETD6 or GST protein (negative control) diluted in 1% BSA in PBST for 1 hr at RT. Plates were then washed and incubated with primary antibody (anti-GST, 1:4000 dilution) followed by incubation with HRP-conjugated secondary antibody (goat anti-rabbit, 1:2000 dilution) for 1 hr. Finally, TMB reagent and then 1N H2SO4 were added; the absorbance at 450 nm was detected using a Tecan Infinite M200 plate reader. Results are represented as relative absorbance fold compared to GST or BSA\ His-Sumo.

## Mass spectrometry analysis

*In vitro* methylation reaction was performed as described above, but instead of using a radioactive SAM, 300 μM non-radioactive SAM was added (Abcam, ab142221). Reactions were then sent for mass spectrometry analysis at Weizmann Institute of Science as described previously (32).

## Antibodies and Western blot Analysis

Samples were denatured with Laemmli sample buffer (250mM Tris-HCl pH 6.8, 10% SDS, 30% glycerol, 5% β-mercaptoethanol, a pinch of bromophenolblue), boiled for 5 min at 95°C, resolved on 8%-12% SDS-PAGE gel, and then blotted onto PVDF membranes. Primary antibodies used were anti-Flag (Sigma, F1804), anti-HA (Millipore, 05–904), anti-actin (Abcam, ab3280), anti-SETD6 (Genetex, GTX629891), anti PPARγ (CST, 2435), anti PPARγ2 (Abcam, ab45036), and anti-histone3 (H3) (Abcam, ab10799), anti PPARγ K170me1 (Abmart Inc.). HRP-conjugated secondary antibodies, goat anti-rabbit, goat anti-mouse, mouse anti-Rabbit were purchased from Jackson ImmunoResearch (111-035-144, 115-035-062, 211-032-171 respectively). For endogenic immunoprecipitation of the SETD6 experiment, HRP Goat anti-mouse light chain antibody (Jackson, 115-035-174) was used. Antibodies were diluted and prepared in TBST with 5% BSA or in PBST with 10% skim milk, according to manufacturer's recommendations. The immobilized HRP antibodies were detected by ECL (Biological Industries). For Western blot analysis, cells were homogenized and lysed in RIPA buffer (50 mM Tris-HCl pH 8, 150 mM NaCl, 1% Nonidet P-40, 0.5% sodium deoxycholate, 0.1% SDS, 1 mM DTT, and 1:100 protease inhibitor mixture (Sigma)). Samples were resolved on SDS-PAGE, followed by Western blot analysis.

## Chromatin Extraction

10cm plate of HepG2 cells washed three times with PBSx1, harvested, and centrifuged (1,800*xg*, 5 min, 4°C). Firstly, the pellet was resuspended with 500ul of Buffer A (10mM Hepes pH 7.9, 10mM KCl, 1.5mM MgCl2, 0.34M Sucrose, and 10% Glycerol) supplemented with 0.1% Triton, 1Mm DTT, 1:200 Protease Inhibitor cocktail (PI), 100Nm PMSF and incubated on ice for 8 minutes. After another centrifugation, the supernatant was removed, and the pellet that consists mainly of intact nuclei was rewashed with Buffer A with the same supplementation without the addition of Triton. Then, the washed pellet was resuspended with 500ul of No Salt Buffer (3mM EDTA, 0.2mM EGTA) supplemented with 1:200 PI cocktail (P8340, Sigma) and 1mM DTT and kept on ice for 30 minutes with occasional vortexing. After centrifugation and removing soluble nuclear proteins from the pellet, the pellet will consist of a chromatin fraction. Two different approaches were carried out to extract the soluble chromatin proteins; in the first one, the chromatin pellet was resuspended with 200ul of Buffer A supplemented with 1:200 PI cocktail (P8340, Sigma) and 1:200 Benzonase (E1014-25KU, Sigma), incubated for 15 minutes at 37°C to solubilize pellet. The second approach included resuspension of the chromatin pellet with 100ul of Buffer A with the addition of 1:200 PI and then sonicated (Bioruptor, Diagenode) at high power settings for 3 cycles, 6 min each (30 sec ON/OFF) (Figure. 20B). The soluble chromatin fraction was collected by low-speed centrifugation (1,800*xg*, 5 min, 4°C).

## Immunoprecipitation (IP)

Preclear of the chromatin fraction for 1hr at RT was conducted with Magnetic CHIP protein A/G magnetic beads (Millipore, 16-663). Afterward, the soluble chromatin fraction was incubated overnight at 4°C with pre-conjugated A/G magnetic beads with an antibody of interest, washed three times with and analyzed by Western blot.

## Dual-Luciferase Assay

HepG2 cells were seeded in 24-well plates and transiently transfected with 0.1 μg Flag-PPARγ WT or K117R mutant, 0.1 μg firefly luciferase plasmid, containing *SETD6* promoter, and 0.1 μg Renilla luciferase plasmid. Total amount of transfected DNA in each dish was kept constant by the addition of empty vector, as necessary. Cell extracts were prepared 24h after transfection, and firefly luciferase activity was measured with the Dual-Glo Luciferase Assay system (Promega) and normalized to that of Renilla luciferase.

## Proximity Ligation Assay (PLA) image processing and data analysis

Cells were cultivated on coated coverslips, washed with PBS and fixed in cold 4% Paraformaldehyde (PFA) at RT for 15min. Cell permeabilization was performed using 0.5% Triton X-100 in PBS for 10min in RT. PLA (Duolink) was performed according to the manufacturer's instructions (Sigma) using antibodies against BRD4 (Bethyl, A700-004), MITF (Santa Cruz, sc-515925) and Flag (Sigma, F1804) overnight in 4°C. Images were acquired by confocal Spinning disk microscopy with a 100x or 63x objective. Each frame represents maximum intensity projection for Z-stacks captured, and 4-6 frames were captured for each sample. with DAPI, using Duolink mounting media). Each nucleus is then represented as a point in the quantification graph. Image processing and data analysis was previously described (33).

## RNA-Sequencing

Total RNA from HepG2 cells was extracted using the NucleoSpin RNA Kit (Macherey-Nagel) according to the manufacturer's instructions. Samples were prepared in two biological replicates for control cells, four biological replicates for SETD6 KO and four biological replicas for PPARγ and PPARγ K170R mutant. Libraries were prepared using the INCPM-mRNA-seq protocol. Briefly, the polyA fraction (mRNA) was purified from 500 ng of total input RNA followed by fragmentation and the generation of double-stranded cDNA. Afterward, an Agencourt Ampure XP beads cleanup (Beckman Coulter), end repair, A base addition, adapter ligation, and PCR amplification steps were performed. Libraries were quantified by Qubit (Thermo fisher scientific) and TapeStation (Agilent). The sequencing was done on a Hiseq instrument (Illumina).

## RNA-Sequencing analysis

The analysis of the raw sequence reads was carried out using the NeatSeq-Flow platform (*https://doi.org/10.1101/173005*). The sequences were quality trimmed and filtered using Trim Galore (version 0.4.5) (quality cutoff=25, length cutoff=25) and cutadapt (version 1.15) (DOI: *https://doi.org/10.14806/ej.17.1.200*). Alignment of the reads to the human genome (GRCh38) was done with RSEM (version 1.2.28) (Li and Dewey, 2011) (option 'bowtie2') and calculation of number of reads per gene per sample was also done with RSEM. Quality assessment of the process was carried out using FASTQC (version 0.11.8) and MultiQC (version 1.0.dev0) (Ewels et al, 2016). Genes with low expression values (mean count < 1 over all samples) were excluded from differential expression analysis. Read counts for differential gene expression were analyzed with the DESeq2 R package (34) using the the NeatSeq-Flow platform DESeq2 module. Genes with fold change ≥ 1 and adjusted P < .05 were considered as significantly differentially expressed genes. Significant genes were clustered using the 'eclust' function from the factorextra R package (10.32614/CRAN.package.factoextra) with the default restriction of maximum clusters. In some cases, batch effect was included in the design and also corrected for visualization purposes using the sva R package (35). sva: Surrogate Variable Analysis. R package version 3.52.0). For treated mutant PPARγ vs. treated WT PPARγ and for treated WT PPARγ vs. EMPTY PPARγ, genes with fold change ≥ 1 and adjusted P < .05. Enrichment for Gene Ontology biological processes and KEGG pathways was performed using clusterProfiler v4.0 R package (doi:10.1016/j.xinn.2021.100141).

## Real-Time qPCR

200 ng of the extracted RNA was reverse transcribed to cDNA using the iScript cDNA Synthesis Kit (Bio-Rad) according to the manufacturer's instructions. Real-time qPCR was performed using the Light cycler 480 SYBR green master (Roche, 04-887-352). All samples were amplified in triplicates in a 384-well plate using the following cycling conditions: 5 min at 95°C, 45 cycles of amplification; 10 sec at 95°C, 10 sec at 60°C, and 10 sec at 72°C, followed by melting curve acquisition; 5 sec at 95°C, 1 min at 65°C and monitoring up to 97°C, and finally cooling for 30 sec at 40°C Gene expression levels were normalized relative to GAPDH gene and controls of the experiment.

## ChIP-qPCR

For DNA ChIP qPCR, DNA ChIP protocol was used from (36) with the following modifications: HepG2 Cells from 10cm plate were cross-linked using 1.5% formaldehyde (Sigma, F8775) on a shaking platform for 10 min at room temperature. The cross-linking reaction was stopped by adding 1.25M glycine pH 8.5 for 5 min at room temperature. Cells were harvested and washed three times with cold phosphate-buffered saline, once with 2.5 ml of buffer I (10 mM HEPES [pH 6.5], 10 mM EDTA, 0.5 mM EGTA, 0.25% Triton X-100), and once with buffer II (10 mM HEPES [pH 6.5], 1 mM EDTA, 0.5 mM EGTA, 200 mM NaCl). Afterward, cells were resuspended with 500ul of lysis buffer (50mM Tris pH 8, 10mM EDTA, 1% SDS, 1:100 Protease Inhibitor cocktail) then sonicated (Bioruptor, Diagenode) at high power settings for 6 cycles, 6 min each (30 sec ON/OFF). The chromatin extract was then clarified by centrifugation for 15 min, full speed at 4°C, and diluted 5x in dilution buffer (20 mM Tris pH 8, 2 mM EDTA, 150 mM NaCl, 1.84% Triton X-100, and 0.2% SDS). Chromatin immunoprecipitation was performed as previously described (36,37). Chromatin was precleared overnight at 4°C with Magnetic CHIP protein A/G magnetic beads (Millipore, 16-663). The precleared sample was then immunoprecipitated in dilution buffer with Anti FLAG magnetic beads (Sigma, M8823) or Magnetic CHIP protein A/G magnetic beads (Millipore, 16-663). The immunoprecipitated complexes were washed once with TSE150 buffer (20 mM Tris pH 8, 2 mM EDTA, 1% Triton X-100, 0.1% SDS and 150 mM NaCl), TSE500 buffer (20 mM Tris pH 8, 2 mM EDTA, 1% Triton X-100, 0.1% SDS and 500 mM NaCl) buffer 3 (250 mM LiCl, 10 mM Tris pH 8, 1 mM EDTA, 1% sodium deoxycholate and 1% Nonidet P-40), and twice with TE buffer (10 mM Tris pH 8 and 1 mM EDTA). DNA was eluted with elution buffer (50 mM NaHCO3, 140 mM NaCl and 1% SDS) containing 0.2 µg/µl RNase A and 0.2 µg/µl Proteinase K. Finally, the DNA eluates were decross-linked at 65°C overnight with shaking at 900 rpm and purified by NucleoSpin Gel and PCR Clean-up kit (Macherey-Nagel), according to manufacturer's instructions. Purified DNA was subjected to qPCR using specific primers (Table 3). Primers were designed based on PPARγ occupancy as previously described on PPARγ target gene (38,39). qPCR was performed using SYBR Green I Master (Roche) in a LightCycler 480 System (Roche). All samples were amplified in five replicates in a 384-well plate using the following cycling conditions: 5 min at 95°C, 45 cycles of amplification; 10 sec at 95°C, 10 sec at 60°C, and 10 sec at 72°C, followed by melting curve acquisition; 5 sec at 95°C, 1 min at 65°C and monitoring up to 97°C, and finally cooling for 30 sec at 40°C. The results were normalized to input DNA and presented as % input.

| Name | Sequence (5' to 3') |
|---|---|
| Mogat1 PPRE Fw | GAGCTCTTCTTGGAGTTCAGCC |
| Mogat1 PPRE Rev | GCCCTTACTTGAGCTGTAGCC |
| PLIN2 PPRE Fw | CCTGCTCTAATGACCTCTTACTTTGC |
| PLIN2 PPRE Rev | CCTTAAGTGAGGAAATGACTCACAGG |
| SETD6 promoter PPRE region I FW | CTGGCAAATAAGGGCAGAGG |
| SETD6 promoter PPRE region I Rev | GAGCGACCTCCTGATCTCGAC |

**Table 3. Primers for ChIP – qPCR**

## Lipid Droplet Dynamics with Live Imaging microscopy

$20\times 10^3$ cells of HepG2 cells were plated in 48 plate-well. On the next day, a live imaging microscopy was conducted for 20 or 24 hours to measure Oleic Acid (OA) accumulation. For Lipid Droplets biogenesis, cells were treated with 600 µmol/l of oleic acid [(OA, conjugated to albumin at 5:1 mol/l ratio), Sigma-Aldrich, St. Louis, MO, USA], with 200 ng/ml BODIPY 493/503 (D3922; Invitrogen, Carlsbad, CA, USA) for neutral lipid staining and 1 µg/ml Hoechst 33342 (H1399;

Thermo Fisher Scientific, Inc., Waltham, MA, USA) was added for staining nuclei immediately before imaging. Imaging experiments were taken using a LionHeart FX (BioTek Instruments) configured with DAPI, GFP, and Brightfield light cubes. The fluorescence was measured with a 10x objective area scan with 3 beacons for each well and averaging the GFP signal for each well to account for variations in cell location in the well. Differences in cell number were corrected by using Hoechst fluorescence to normalize the BODIPY signal in each well. Data represents the mean of 3 wells per treatment. Image Analysis used primary and secondary masks of the captured digital images to determine the Mean GFP which represents the mean OA accumulation per cell. Primary mask analysis of the DAPI channel identifies individual cells by their nuclei. The secondary mask is denoted as the region up to 20 µm surrounding each nucleus and represents the cytoplasmic cell region. Scale bar indicates 200 µm.

### Statistical Analyses

Statistical analyses for all assays were analyzed with GraphPad Prism software, using Student's two-tailed t-test (unpaired) when comparing two groups or one-way analysis of variance (ANOVA) with a Tukey's *post hoc* test for comparing more than two groups. Two-way ANOVA was performed when two different categorical independent variables were tested on one dependent variable.

## Supplementary figures

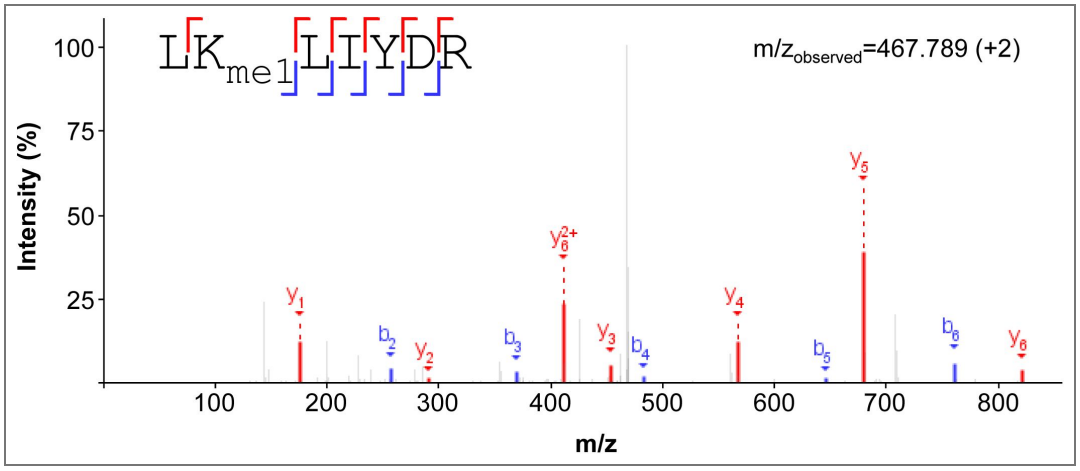


**Fig S1. MS/MS spectra showing monomethylation of recombinant PPARγ at lysine-170 (LKme1LIYDR, m/zobserved =467.789 (z=+2)) after in vitro methylation by SETD6.** The MS spectra was visualized with PDV software (v.2.0.0 (40). The y– and b-ions are annotated and displayed as red, and blue, respectively.

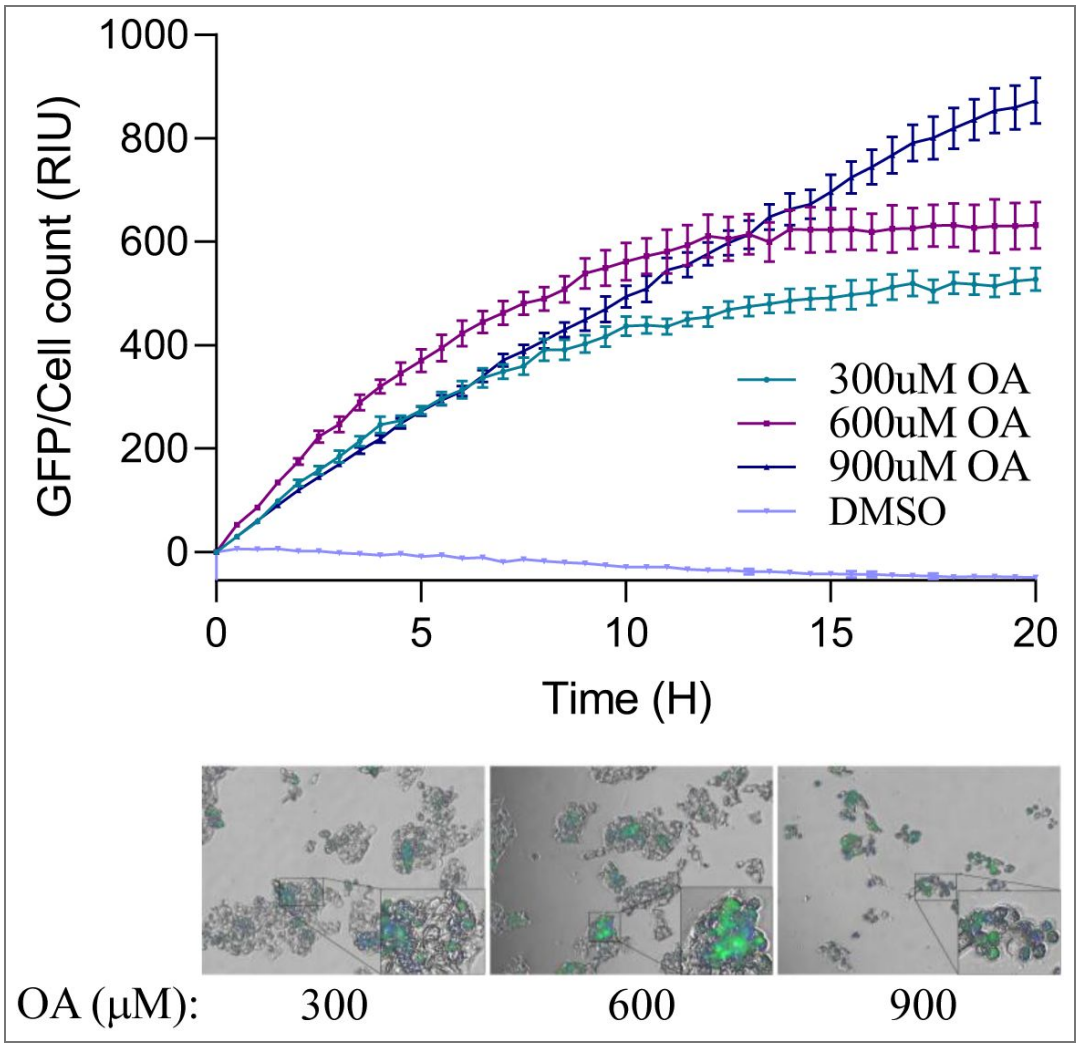


**Fig S2. Top: OA accumulation curve of HepG2 cells over 20 hours challenged with 300 μM, 600 μM, and 900 μM of OA.** 900 μM DMSO served as a control treatment. Mean green fluorescence was calculated as fluorescence signal divided by cell count. Data is analyzed from five beacons per well, with three wells per OA or DMSO treatment. Bottom-Representative images of last time point (20 H) with three concentrations of OA. For each image, a magnified area of interest is shown (black boxes).

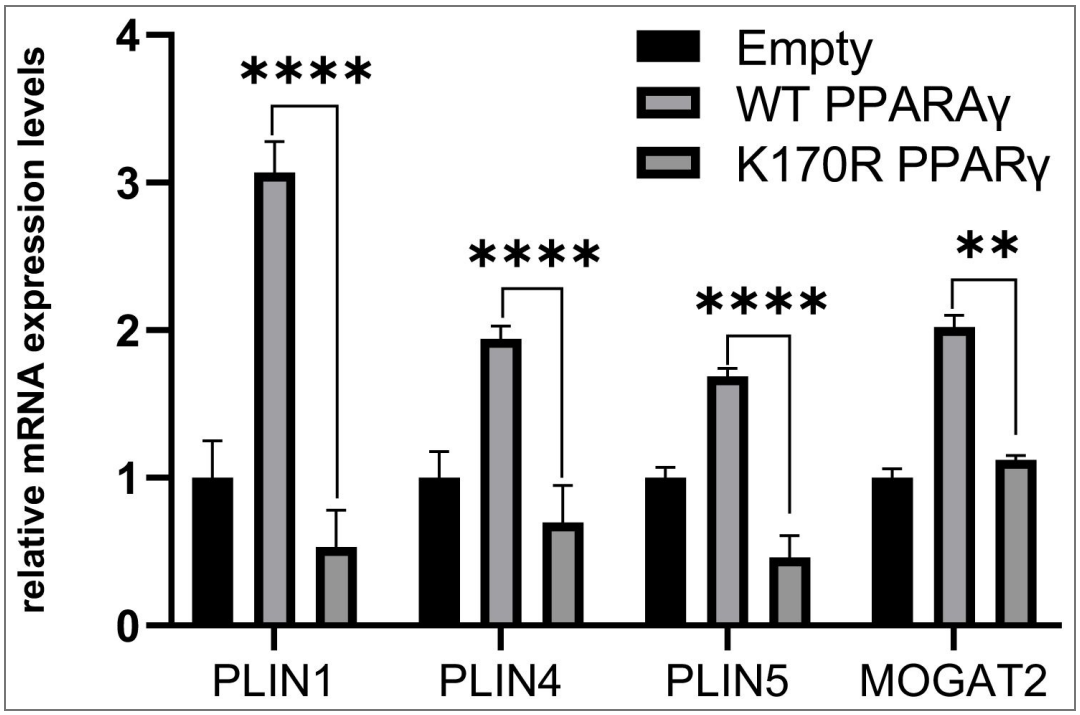


**Fig S3. Transcript levels of the indicated genes were determined by qPCR of stably expressing HepG2 cells-Empty, Flag-PPARγ WT, and Flag-PPARγ K170R mutant.** mRNA levels were normalized to GAPDH and then to Empty. error bars are S.E.M. ***p* < 0.01; ****p < 0.0001*.

## Data availability

RNA sequence data will be deposited to GEO

## Acknowledgements

This work was supported by grants to DL from The Israel Science Foundation (262/18 and 496/23), The Research Career Development Award from the Israel Cancer Research Fund and from the Israel Cancer Association.

## Additional information

### Author Contribution

N.N. and D.L. conceived and designed the study. N.N., D.G., and M.A. performed the majority of the experiments and analyzed the data. A.C. performed the mass spectrometry analysis. M.F. performed the PLA experiments. Y.H., H.M., and A.R. contributed to data interpretation and provided conceptual input. D.L. wrote the manuscript with input from all authors. All authors reviewed and approved the final version of the manuscript.

### Author ORCID iDs

**Dan Levy**: https://orcid.org/0000-0003-0719-0305

## References

1. **Younossi Z.M.,** Koenig A.B., Abdelatif D., Fazel Y., Henry L., Wymer M (2016) Global epidemiology of nonalcoholic fatty liver disease-Meta-analytic assessment of prevalence, incidence, and outcomes. *Hepatology* **64**:73-84 https://doi.org/10.1002/hep.28431 | PubMed

2. **Albert M.,** Helin K (2010) Histone methyltransferases in cancer. *Semin Cell Dev Biol* **21**:209-220 https://doi.org/10.1016/j.semcdb.2009.10.007 | PubMed

3. **Shi Y.,** Whetstine J.R (2007) Dynamic regulation of histone lysine methylation by demethylases. *Mol Cell* **25**:1-14 https://doi.org/10.1016/j.molcel.2006.12.010 | PubMed

4. **Chopra A.,** Feldman M., Levy D (2025) Orchestrating epigenetics: a comprehensive review of the methyltransferase SETD6. *Exp Mol Med* **57**:533-544 https://doi.org/10.1038/s12276-025-01423-2 | PubMed

5. **Evans R.M.,** Barish G.D., Wang Y.X (2004) PPARs and the complex journey to obesity. *Nat Med* **10**:355-361 https://doi.org/10.1038/nm1025 | PubMed

6. **Wang Y.X** (2010) PPARs: diverse regulators in energy metabolism and metabolic diseases. *Cell Res* **20**:124-137 https://doi.org/10.1038/cr.2010.13 | PubMed

7. **Li Z.,** Luo L., Yu W., Li P., Ou D., Liu J., Ma H., Sun Q., Liang A., Huang C., *et al.* (2022) PPARgamma phase separates with RXRalpha at PPREs to regulate target gene expression. *Cell Discov* **8**:37 https://doi.org/10.1038/s41421-022-00388-0 | PubMed

8. **Wang Y.,** Nakajima T., Gonzalez F.J., Tanaka N (2020) PPARs as Metabolic Regulators in the Liver: Lessons from Liver-Specific PPAR-Null Mice. *Int J Mol Sci* **21** https://doi.org/10.3390/ijms21062061 | PubMed

9. **Manickam R.,** Wahli W (2017) Roles of Peroxisome Proliferator-Activated Receptor beta/delta in skeletal muscle physiology. *Biochimie* **136**:42-48 https://doi.org/10.1016/j.biochi.2016.11.010 | PubMed

10. **Zingarelli B.,** Piraino G., Hake P.W., O'Connor M., Denenberg A., Fan H., Cook J.A (2010) Peroxisome proliferator-activated receptor {delta} regulates inflammation via NF-{kappa}B signaling in polymicrobial sepsis. *Am J Pathol* **177**:1834-1847 https://doi.org/10.2353/ajpath.2010.091010 | PubMed

11. **Lee Y.K.,** Park J.E., Lee M., Hardwick J.P (2018) Hepatic lipid homeostasis by peroxisome proliferator-activated receptor gamma 2. *Liver Res* **2**:209-215 https://doi.org/10.1016/j.livres.2018.12.001 | PubMed

12. **Jetton T.L.,** Flores-Bringas P., Leahy J.L., Gupta D (2021) SetD7 (Set7/9) is a novel target of PPARgamma that promotes the adaptive pancreatic beta-cell glycemic response. *J Biol Chem* **297**:101250 https://doi.org/10.1016/j.jbc.2021.101250 | PubMed

13. **Fornes O.,** Castro-Mondragon J.A., Khan A., van der Lee R., Zhang X., Richmond P.A., Modi B.P., Correard S., Gheorghe M., Baranasic D., *et al.* (2020) JASPAR 2020: update of the open-access database of transcription factor binding profiles. *Nucleic Acids Res* **48**:D87-D92 https://doi.org/10.1093/nar/gkz1001 | PubMed

14. **Zheng R.,** Wan C., Mei S., Qin Q., Wu Q., Sun H., Chen C.H., Brown M., Zhang X., Meyer C.A., *et al.* (2019) Cistrome Data Browser: expanded datasets and new tools for gene regulatory analysis. *Nucleic Acids Res* **47**:D729-D735 https://doi.org/10.1093/nar/gky1094 | PubMed

15. **Mogilenko D.A.,** Shavva V.S., Dizhe E.B., Orlov S.V., Perevozchikov A.P (2010) PPARgamma activates ABCA1 gene transcription but reduces the level of ABCA1 protein in HepG2 cells. *Biochem Biophys Res Commun* **402**:477-482 https://doi.org/10.1016/j.bbrc.2010.10.053 | PubMed

16. **Kublanovsky M.,** Ulu G.T., Weirich S., Levy N., Feldman M., Jeltsch A., Levy D (2023) Methylation of the transcription factor E2F1 by SETD6 regulates SETD6 expression via a positive feedback mechanism. *J Biol Chem* **299**:105236 https://doi.org/10.1016/j.jbc.2023.105236 | PubMed

17. **Levy D.,** Kuo A.J., Chang Y., Schaefer U., Kitson C., Cheung P., Espejo A., Zee B.M., Liu C.L., Tangsombatvisit S., *et al.* (2011) Lysine methylation of the NF-kappaB subunit RelA by SETD6 couples activity of the histone methyltransferase GLP at chromatin to tonic repression of NF-kappaB signaling. *Nat Immunol* **12**:29-36 https://doi.org/10.1038/ni.1968 | PubMed

18. **Chang Y.,** Levy D., Horton J.R., Peng J., Zhang X., Gozani O., Cheng X (2011) Structural basis of SETD6-mediated regulation of the NF-kB network via methyl-lysine signaling. *Nucleic Acids Res* **39**:6380-6389 https://doi.org/10.1093/nar/gkr256 | PubMed

19. **Qiu B.,** Simon M.C (2016) BODIPY 493/503 Staining of Neutral Lipid Droplets for Microscopy and Quantification by Flow Cytometry. *Bio Protoc* **6** https://doi.org/10.21769/bioprotoc.1912 | PubMed

20. **Soufi N.,** Hall A.M., Chen Z., Yoshino J., Collier S.L., Mathews J.C., Brunt E.M., Albert C.J., Graham M.J., Ford D.A., *et al.* (2014) Inhibiting monoacylglycerol acyltransferase 1 ameliorates hepatic metabolic abnormalities but not inflammation and injury in mice. *J Biol Chem* **289**:30177-30188 https://doi.org/10.1074/jbc.m114.595850 | PubMed

21. **Tsai T.H.,** Chen E., Li L., Saha P., Lee H.J., Huang L.S., Shelness G.S., Chan L., Chang B.H (2017) The constitutive lipid droplet protein PLIN2 regulates autophagy in liver. *Autophagy* **13**:1130-1144 https://doi.org/10.1080/15548627.2017.1319544 | PubMed

22. **Malodobra-Mazur M.,** Oldakowska M., Dobosz T (2024) Exploring PPAR Gamma and PPAR Alpha's Regulation Role in Metabolism via Epigenetics Mechanism. *Biomolecules* **14** https://doi.org/10.3390/biom14111445 | PubMed

23. **Yin L.,** Wang L., Shi Z., Ji X., Liu L (2022) The Role of Peroxisome Proliferator-Activated Receptor Gamma and Atherosclerosis: Post-translational Modification and Selective Modulators. *Front Physiol* **13**:826811 https://doi.org/10.3389/fphys.2022.826811 | PubMed

24. **Brunmeir R.,** Xu F (2018) Functional Regulation of PPARs through Post-Translational Modifications. *Int J Mol Sci* **19** https://doi.org/10.3390/ijms19061738 | PubMed

25. **Diezko R.,** Suske G (2013) Ligand binding reduces SUMOylation of the peroxisome proliferator-activated receptor gamma (PPARgamma) activation function 1 (AF1) domain. *PLoS One* **8**:e66947 https://doi.org/10.1371/journal.pone.0066947 | PubMed

26. **Choi S.,** Jung J.E., Yang Y.R., Kim E.S., Jang H.J., Kim E.K., Kim I.S., Lee J.Y., Kim J.K., Seo J.K., *et al.* (2015) Novel phosphorylation of PPARgamma ameliorates obesity-induced adipose tissue inflammation and improves insulin sensitivity. *Cell Signal* **27**:2488-2495 https://doi.org/10.1016/j.cellsig.2015.09.009 | PubMed

27. **Li Y.,** Wei X., Xiao R., Chen Y., Xiong T., Fang Z.M., Huo B., Guo X., Luo H., Wu X., *et al.* (2024) SMYD2-Methylated PPARgamma Facilitates Hypoxia-Induced Pulmonary Hypertension by Activating Mitophagy. *Circ Res* **135**:93-109 https://doi.org/10.1161/circresaha.124.323698 | PubMed

28. **Itabe H.,** Yamaguchi T., Nimura S., Sasabe N (2017) Perilipins: a diversity of intracellular lipid droplet proteins. *Lipids Health Dis* **16**:83 https://doi.org/10.1186/s12944-017-0473-y | PubMed

29. **Yen C.L.,** Stone S.J., Cases S., Zhou P., Farese R.V. (2002) Identification of a gene encoding MGAT1, a monoacylglycerol acyltransferase. *Proc Natl Acad Sci U S A* **99**:8512-8517 https://doi.org/10.1073/pnas.132274899 | PubMed

30. **Yang N.,** Wang Y., Tian Q., Wang Q., Lu Y., Sun L., Wang S., Bei Y., Ji J., Zhou H., *et al.* (2023) Blockage of PPARgamma T166 phosphorylation enhances the inducibility of beige adipocytes and improves metabolic dysfunctions. *Cell Death Differ* **30**:766-778 https://doi.org/10.1038/s41418-022-01077-x | PubMed

31. **Martin-Morales L.,** Feldman M., Vershinin Z., Garre P., Caldes T., Levy D (2017) SETD6 dominant negative mutation in familial colorectal cancer type X. *Hum Mol Genet* **26**:4481-4493 https://doi.org/10.1093/hmg/ddx336 | PubMed

32. **Admoni-Elisha L.,** Elbaz T., Chopra A., Shapira G., Bedford M.T., Fry C.J., Shomron N., Biggar K., Feldman M., Levy D (2022) TWIST1 methylation by SETD6 selectively antagonizes LINC-PINT expression in glioma. *Nucleic Acids Res* **50**:6903-6918 https://doi.org/10.1093/nar/gkac485 | PubMed

33. **Biton T.E.,** Feldman M., Davidy T., Moskovitz N.T., Levin L., Sevilla D., Goding C.R., Bernstein E., Levy D (2025) SETD6 mediates selective interaction and genomic occupancy of BRD4 and MITF in melanoma cells. *NAR Cancer* **7**:zcaf023 https://doi.org/10.1093/narcan/zcaf023 | PubMed

34. **Love M.I.,** Huber W., Anders S (2014) Moderated estimation of fold change and dispersion for RNA-seq data with DESeq2. *Genome Biol* **15**:550 https://doi.org/10.1186/s13059-014-0550-8 | PubMed

35. **Leek J.T.,** Johnson W.E., Parker H.S., Jaffe A.E., Storey J.D (2012) The sva package for removing batch effects and other unwanted variation in high-throughput experiments. *Bioinformatics* **28**:882-883 https://doi.org/10.1093/bioinformatics/bts034 | PubMed

36. **Ainbinder E.,** Revach M., Wolstein O., Moshonov S., Diamant N., Dikstein R (2002) Mechanism of rapid transcriptional induction of tumor necrosis factor alpha-responsive genes by NF-kappaB. *Mol Cell Biol* **22**:6354-6362 https://doi.org/10.1128/mcb.22.18.6354-6362.2002 | PubMed

37. **Mishra S.,** Van Rechem C., Pal S., Clarke T.L., Chakraborty D., Mahan S.D., Black J.C., Murphy S.E., Lawrence M.S., Daniels D.L., *et al.* (2018) Cross-talk between Lysine-Modifying Enzymes Controls Site-Specific DNA Amplifications. *Cell* **174**:803-817. https://doi.org/10.1016/j.cell.2018.06.018 | PubMed

38. **Yu J.H.,** Lee Y.J., Kim H.J., Choi H., Choi Y., Seok J.W., Kim J.W (2015) Monoacylglycerol O-acyltransferase 1 is regulated by peroxisome proliferator-activated receptor gamma in human hepatocytes and increases lipid accumulation. *Biochem Biophys Res Commun* **460**:715-720 https://doi.org/10.1016/j.bbrc.2015.03.095

39. **Tachibana K.,** Kobayashi Y., Tanaka T., Tagami M., Sugiyama A., Katayama T., Ueda C., Yamasaki D., Ishimoto K., Sumitomo M., *et al.* (2005) Gene expression profiling of potential peroxisome proliferator-activated receptor (PPAR) target genes in human hepatoblastoma cell lines inducibly expressing different PPAR isoforms. *Nucl Recept* **3**:3 https://doi.org/10.1186/1478-1336-3-3 | PubMed

40. **Li K.,** Vaudel M., Zhang B., Ren Y., Wen B (2019) PDV: an integrative proteomics data viewer. *Bioinformatics* **35**:1249-1251 https://doi.org/10.1093/bioinformatics/bty770 | PubMed

# Peer reviews

## Reviewer #1 (Public review):

Summary:

In this manuscript from the Levy lab, the authors investigate whether SETD6 regulates hepatic lipid accumulation through direct methylation of PPARγ. They show that SETD6 binds and mono-methylates PPARγ at K170, and provide evidence that this modification enhances PPARγ occupancy at target promoters, promotes expression of lipid metabolism genes, as well as facilitates lipid droplet accumulation in HepG2 cells. The authors also find a positive feedback loop or circuit in which PPARγ activates SETD6 transcription in a methylation-dependent manner, thereby reinforcing this lipogenic program. Overall, the work presents a novel SETD6-PPARγ regulatory axis linking lysine methylation to transcriptional control of lipid storage genes, with possible relevance to NAFLD-associated biology.

In all, I find this to be an important paper that describes and advances a new regulatory pathway that has significance to human health and disease. It would also be of interest to a broad audience. That said, there are also some concerns that the authors should address, as outlined below.

Major concerns (pertains to rigor - highest priority)

(1) Overall, the work presented is of high quality, and the data nicely support the conclusions; however, a few panels should be strengthened that have missing controls or information:

a. The co-IP panel in Figure 1B lacks a lane where HA SETD6 is expressed without PPARγ. This control is needed to verify that the SEDT6-HA signal depends on PPARγ.

b. In Figure 1C, the authors should show that the co-IP works in both directions (include IP for PPARγ/blot for SETD6). I am a bit confused also over the labeling with IP on the left and on top of the panel next to the beads label. More importantly, the data would be stronger if the

authors took advantage of a deletion line to validate that the co-IP is specific to the presence of both.

c. The same IP labeling issue exists for Figure 3B (label is on the same and on top).

d. Antibody information (e.g., where the pan-methyl Ab comes from and at what dilutions they are used at) is missing.

Nice to have experiments (medium priority - strongly consider)

(2) A missing gap is how K170me1 contributes to DNA binding and gene transcription. One possibility is that methylation enhances the DNA-binding activity of PPARγ. Given that the authors have all of the reagents, it would be possible to perform a gel shift assay (or other approach) with and without SETD6-mediated methylation. Is DNA binding affected/enhanced?

(3) Along these lines, I wonder if there is another possibility: could SETD6-mediated methylation of PPARγ drive SETD6-PPARγ interaction? In other words, in the K170R, is SETD6 still even associated with PPARγ, and this interaction is required for promoter recruitment? Alternatively, would a catalytic dead version of SETD6 fail to associate with PPARγ? Currently, no experiments test the impact of an unmethylatable version of PPARγ or a catalytic dead version of SETD6 on SETD6-PPARγ interaction or SETD6 recruitment to promoters.

Minor concerns (text and figure display)

(4) The text has multiple typos and grammatical errors, and there are some issues with the figure display.

https://doi.org/10.7554/eLife.111542.1.sa1

## Reviewer #2 (Public review):

Summary:

In this work, the authors investigated the regulation of the transcription factor PPARγ by the post-translational modification lysine methylation. The data demonstrate that the lysine methyltransferase SETD6 targets PPARγ for methylation using biochemical and cell-based assays. Methylation of PPARγ occurs in its DNA binding domain, and the authors demonstrate that loss of methylation limits PPARγ chromatin binding, particularly to lipid storage and metabolism gene promoters. As a physiological output, the authors demonstrate that deletion of SETD6 and loss of PPARγ methylation also disrupt lipid droplet accumulation in hepatocytes. In addition, the authors uncover a positive feedback loop in which SETD6 methylation of PPARγ also regulates its binding to the SETD6 promoter and expression of the gene.

Strengths:

One of the key strengths of this manuscript is the novelty of the findings in terms of identifying a new mode of regulation of PPARγ that modulates its chromatin association in cells and thereby regulates lipid metabolism genes. The authors nicely combine biochemical studies of SETD6 activity with cell-based assays investigating PPARγ and SETD6 function in regulating lipid storage. Data supporting this conclusion is largely convincing, and frequently, multiple assays are used to provide sufficient support to the conclusions. This work therefore expands regulatory modes of PPARγ and identifies a new target for SETD6, an enzyme that targets a number of other transcription factors. Furthermore, the regulatory loop that controls SETD6 expression via PPARγ methylation is likely important for understanding SETD6 function in different cell types that have high levels of lipid accumulation or

regulation. The gene expression and lipid accumulation assays are useful for testing the physiological outcome of loss of SETD6 activity or PPARγ methylation directly.

Weaknesses:

The data presented in the manuscript are largely convincing in support of the authors' conclusions; however, there are some errors in the presentation of the figures and some issues in the text that would benefit from editing. Furthermore, there are some important questions not fully addressed in the results or discussion. It would be great if the authors could speculate more on the diverse roles of SETD6 in methylated transcription factors and/or provide more context regarding the conditions that are likely to support methylation of PPARγ by SETD6. Also, while a potential cross-talk between methylation and phosphorylation is described in the discussion, it would be great to provide more structural insight into how this might regulate DNA binding of PPARγ and/or discuss whether there are other possibilities given the location of the target lysine in the DNA binding domain.

https://doi.org/10.7554/eLife.111542.1.sa0